Structural Eng. / Earthquake Eng. Vol. 7. No. 1, 179s-188s. April 1990
Japan Society of Civil Engineers (Proc. of JSCE No. 416/I-13)

OPTIMAL CONTROL OF SEISMIC RESPONSE OF STRUCTURES

By Tadanobu SATO, Kenzo TOKI** and Kazuhisa SUGIYAMA****

A new closed-open-loop optimal control algorithm is proposed that has been derived by minimizing the sum of the quadratic time-dependent performance index and the seismic energy input to the structural system. This new control law provides feasible control algorithms that can easily be implemented for applications to seismic-excited structures. We developed optimal control algorithms, taking into account the nonlinearity of the structural system and the effect of the time delay, for applying a control force to a structural system subjected to general dynamic loads. These optimal algorithms are simple and reliable for on-line control operations and effective for a structural system with a base isolation mechanism. The control efficiency affected by two weighting matrices included in the performance index is investigated in detail. Numerical examples are worked out to demonstrate the control efficiency of the proposed algorithms.

Keywords: active control, nonlinear system, time delay, base isolation, weighting matrices

1. INTRODUCTION

The problem of earthquake-induced vibration of tall buildings and long-span bridges is of prime concern to structural engineers. Control of such large, flexible structures by the use of active control forces is a recent area of research in civil engineering. Most of active control algorithms aim to find a feedback control law[1].

The control of earthquake-excited structures is a unique problem in the specialty area of active control. Classical active control theories of structures were applications of optimal regulator problems. Every regulator problem is converted into a feedback optimized with respect to a quadratic performance index that includes product terms between the state and control values[2]. The feedback, therefore, does not include the non-homogeneous term that is a result of the earthquake excitation. Furthermore, the performance index is given by the integration of quadratic evaluation functions over the time interval from 0 to t_f, a duration defined as longer than that of the earthquake; consequently, the input excitation in that interval must be known a priori in order to calculate the state and control values.

Linear control laws are derived for open-loop and open-closed loop control schemes; but, the closed-loop control algorithms are widely used for earthquake-excited structures. This is the special case in which the control force is regulated by the response state vector and the Riccati matrix. It has been pointed out that because external excitation is ignored in the derivation of the Riccati equation, the closed-loop control law is not truly optimal. If the excitation term is included in the Riccati equation, its solution requires a priori knowledge of the loading history. This generally is not possible for excitations

* Member of JSCE, Dr. Eng., Associate Professor, Disaster Prevention Research Institute, Kyoto University (Uji, Kyoto 611, Japan)
** Member of JSCE, Dr. Eng., Professor, Disaster Prevention Research Institute, Kyoto University (Ujij, Kyoto 611, Japan)
*** Engineer, Obayashi-gumi Co. Ltd. (Chiyodaku, Tokyo 101, Japan)

such as earthquakes. To overcome this difficulty several control algorithms have been proposed ; the pole assignment method[3], the instantaneous optimal control[4], and the pulse control[5].

We here propose a new instantaneous closed-open-loop control which takes into account the energy of earthquake motion input to the structure. A time-dependent performance index similar to that defined in Ref. 4) is used to obtain the control vector. The instantaneous optimal control algorithms proposed in Ref. 4) were classified as open-loop, closed-loop and open-closed-loop controls ; but, the control efficiencies were identical because the same performance index was minimized. This is referred to as Yang's optimal control algorithm. We have defined a new objective function of which minimization results in different efficiencies for the three control algorithms.

2. CONTROL ALGORITHM TAKING INTO ACCOUNT INPUT SEISMIC ENERGY

A structure that is idealized by an n-degree of freedom system is subjected to a one-dimensional earthquake ground acceleration $\ddot{X}_0(t)$. The matrix equation of motion is expressed as

$$\boldsymbol{M}\ddot{\boldsymbol{x}}(t)+\boldsymbol{C}\dot{\boldsymbol{x}}(t)+\boldsymbol{K}\boldsymbol{x}(t)=-\boldsymbol{m}\ddot{X}_0(t)+\boldsymbol{H}\boldsymbol{u}(t) \quad (1)$$

in which $\boldsymbol{M}$, $\boldsymbol{C}$, $\boldsymbol{K}$ are the mass, damping and stiffness matrices, $\boldsymbol{u}$ the r-dimensional control vector, and $\boldsymbol{H}$ a $(n\times r)$ matrix specifying the location of active controllers.

The state space description of Eq. (1) is given by

$$\dot{\boldsymbol{z}}(t)=\boldsymbol{A}\boldsymbol{z}(t)+\boldsymbol{B}\boldsymbol{u}(t)+\boldsymbol{W}_1\ddot{X}_0(t) \quad (2)$$

in which

$$\boldsymbol{z}=\begin{Bmatrix} \boldsymbol{x} \\ \dot{\boldsymbol{x}} \end{Bmatrix},\quad \boldsymbol{A}=\begin{bmatrix} \boldsymbol{0} & \boldsymbol{I} \\ -\boldsymbol{M}^{-1}\boldsymbol{K} & -\boldsymbol{M}^{-1}\boldsymbol{C} \end{bmatrix},\quad \boldsymbol{B}=\begin{bmatrix} \boldsymbol{0} \\ \boldsymbol{M}^{-1}\boldsymbol{H} \end{bmatrix},\quad \boldsymbol{W}_1=\begin{bmatrix} \boldsymbol{0} \\ -\boldsymbol{M}^{-1}\boldsymbol{m} \end{bmatrix} \quad (3)$$

The solution of Eq. (2) is

$$\boldsymbol{z}(t)=e^{A\Delta t}\boldsymbol{z}(t-\Delta t)+e^{At}\int_{t-\Delta t}^{t}\{\boldsymbol{B}\boldsymbol{u}(\tau)+\boldsymbol{W}_1\ddot{X}_0(\tau)\}e^{-A\tau}d\tau \quad (4)$$

Using a trapezoidal approximation for the integral term, $\boldsymbol{z}(t)$ is rewritten

$$\boldsymbol{z}(t)=\boldsymbol{D}(t-\Delta t)+\frac{\Delta t}{2}[\boldsymbol{B}\boldsymbol{u}(t)+\boldsymbol{W}_1\ddot{X}_0(t)] \quad (5)$$

in which

$$\boldsymbol{D}(t-\Delta t)=e^{A\Delta t}\left\{\boldsymbol{z}(t-\Delta t)+\frac{\Delta t}{2}[\boldsymbol{B}\boldsymbol{u}(t-\Delta t)+\boldsymbol{W}_1\ddot{X}_0(t-\Delta t)]\right\} \quad (6)$$

To take into account the seismic energy input into the structure, the following integration formula of equation of motion is considered

$$\int_0^t \dot{\boldsymbol{x}}'(\tau)\boldsymbol{M}\ddot{\boldsymbol{x}}(\tau)d\tau+\int_0^t \dot{\boldsymbol{x}}'(\tau)\boldsymbol{C}\dot{\boldsymbol{x}}(\tau)d\tau+\int_0^t \dot{\boldsymbol{x}}'(\tau)\boldsymbol{K}\boldsymbol{x}(\tau)d\tau+\int_0^t \dot{\boldsymbol{x}}'(\tau)\boldsymbol{m}\ddot{X}_0(\tau)d\tau$$
$$=\int_0^t \dot{\boldsymbol{x}}'(\tau)\boldsymbol{H}\boldsymbol{u}(\tau)d\tau \quad (7)$$

The first term on the left side of this equation is the kinetic energy of the system represented by $1/2\,\dot{\boldsymbol{x}}'(t)\boldsymbol{M}\dot{\boldsymbol{x}}(t)$, the second the energy absorbed by system damping, the third the strain energy, and the fourth the total seismic energy input to the structure system. The right hand is the total energy input by the control force.

By segmenting the integration into the time regions $(0\sim t-\Delta t)$ and $(t-\Delta t\sim t)$, Eq. (7) is decomposed into the term related to the values at time t and between $0\sim t-\Delta t$

$$\frac{1}{2}\dot{\boldsymbol{x}}'(t)\boldsymbol{M}\dot{\boldsymbol{x}}(t)+\frac{\Delta t}{2}\dot{\boldsymbol{x}}'(t)\boldsymbol{C}\dot{\boldsymbol{x}}(t)+\frac{\Delta t}{2}\dot{\boldsymbol{x}}'(t)\boldsymbol{K}\boldsymbol{x}(t)+\frac{\Delta t}{2}\dot{\boldsymbol{x}}'(t)\boldsymbol{m}\ddot{X}_0(t)+\boldsymbol{E}(t-\Delta t)$$
$$=\int_0^t \dot{\boldsymbol{x}}'(\tau)\boldsymbol{H}\boldsymbol{u}(\tau)d\tau \quad (8)$$

in which $\boldsymbol{E}(t-\Delta t)$ is the term related to values within the interval $(0\sim t-\Delta t)$.

A new optimal control algorithm can be established by following the time-dependent performance index $J(t)$

$$J(t)=z'(t)Q_1z(t)+u'(t)Ru(t)+\alpha\{z'(t)Q_2z(t)+z'(t)W_2\ddot{X}_0(t)+E(t-\Delta t)\} \quad (9)$$

in which

$$W_2=\{0 \quad m\}', \quad Q_2=\begin{bmatrix} 0 & 0 \\ \frac{\Delta t}{2}K & \frac{\Delta t}{2}C+\frac{1}{2}M \end{bmatrix}$$

To minimize the performance index $J(t)$ given by Eq. (9) under the constraint in Eq. (5), the generalized performance index is defined by

$$\tilde{J}=z'(t)Qz(t)+u'(t)Ru(t)+\alpha\{z'(t)W_2\ddot{X}_0(t)+E(t-\Delta t)\}$$
$$+\Lambda\left[z(t)-D(t-\Delta t)-\frac{\Delta t}{2}\{Bu(t)+W_1\ddot{X}_0(t)\}\right] \quad (10)$$

in which Λ is the Lagrangian multiplier vector and

$Q=Q_1+\alpha Q_2$

The necessary conditions for minimizing the performance index $J(t)$ are

$$\frac{\partial\tilde{J}}{\partial\Lambda}=0, \quad \frac{\partial\tilde{J}}{\partial z}=0, \quad \frac{\partial\tilde{J}}{\partial u}=0 \quad (11\cdot a\sim c)$$

upon substituting Eq. (10) into Eqs. (11·a~c), we obtain

$$2\,Qz(t)+\alpha W_2\ddot{X}_0(t)+\Lambda=0 \quad (12)$$

$$2\,Ru(t)-\frac{\Delta t}{2}B'\Lambda=0 \quad (13)$$

The control vector $u(t)$ can be obtained from Eqs. (12) and (13)

$$u(t)=-\frac{\Delta t}{2}R^{-1}B'Qz(t)-\alpha\frac{\Delta t}{4}R^{-1}B'W_2\ddot{X}_0(t) \quad (14)$$

As seen in Eq. (14) the control vector consists of a feedback of the state at time t and a weighted input ground acceleration at that time; hence, this control law is referred to as the optimal closed-open-loop control. Substituting Eq. (14) into Eq. (5), the state vector $z(t)$ is

$$z(t)=\left[I+\left(\frac{\Delta t}{2}\right)^2 BR^{-1}B'Q\right]^{-1}\cdot\left[D(t-\Delta t)+\frac{\Delta t}{2}\ddot{X}_0(t)\left\{W_1-\alpha\frac{\Delta t}{4}BR^{-1}B'W_2\right\}\right] \quad (15)$$

3. APPLICATION TO LINEAR STRUCTURE

To demonstrate the application of the algorithm, a three-story building was modeled as shown in Fig. 1. The parameters for this model are given in Table 1. Active tendon controllers are assumed to be installed in every story unit. The accelerogram at Taft (S 69 E, July 21, 1952) amplified as the maximum acceleration to 340 gal was used. The respective relative displacements of the top floor for our newly proposed control algorithm, Yang's optimal control[4], and no control are shown in Fig. 2 (a), (b) and (c). The corresponding required control forces from the top and bottom actuators are depicted in Fig. 3 (a) and (b). To check the efficiency of both control algorithms, the same weighting matrices Q and R were used in the calculation of the control forces. The maximum response values are controlled at less than half the value without control. The time history of the control force at the bottom actuator obtained by our algorithm is very similar to the input accelerogram, but with 1.7 times larger maximum control force than that from Yong's optimal control algorithm. The maximum control force at the top actuator, however, is 40 % smaller than that obtained by Yang's algorithm. This means that our proposed algorithm generates a rather large control force for the base controller that corresponds to the input acceleration and reduces the seismic energy input to the upper floors. To make clear this fact the input seismic energy to structure and the total energy being used for controling the structure as well as maximum response values are given in Table 2. Input and control energy of our algorithm are about half the values of Yong's algorithm. The control efficiency of our method is, therefore, better than that of the instantaneous optimal algorithm.

To examine the effects of the weighting matrices Q and R, and parameter α on active control, we considered two different types of Q. To define them we partitioned Q as follows :

$$Q=\begin{bmatrix} Q_{11} & Q_{12} \\ Q_{21} & Q_{22} \end{bmatrix} \quad (16)$$

in which the order of matrices Q_{ij} is (3×3). Note that the submatrices Q_{11} and Q_{12} do not contribute to the active forces because the matrix B which appears in Eq. (3) contains 0 matrix ; therefore, Q_{11} and Q_{12} are designated as zero. For simplicity, Q_{21} and Q_{22} are considered to be equal, and we assigned the unit matrix to R. The appropriate assignment of the elements of Q_{21} and Q_{22} to achieve maximum control efficiency have not been investigated because it requires a two stage optimization technique that is beyond the scope of the research reported here. For illustrative purposes the following two matrices are used

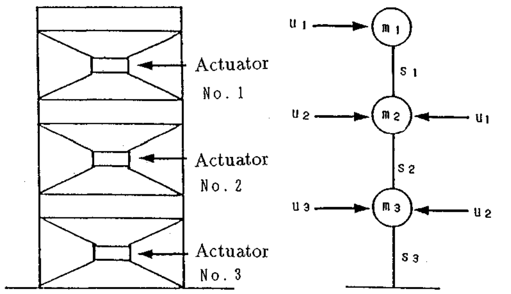

Fig. 1 Model of the structural system.

Table 1 Structural properties of a linear model.

Active tendon Control		
No.	Mass (ton)	Stiffness (tonf/cm)
1	0.048	23.66
2	0.048	42.59
3	0.048	47.32

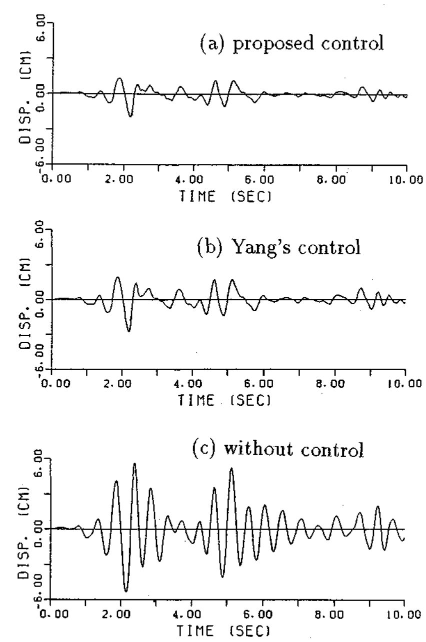

Fig. 2 Relative displacement of the top floor.

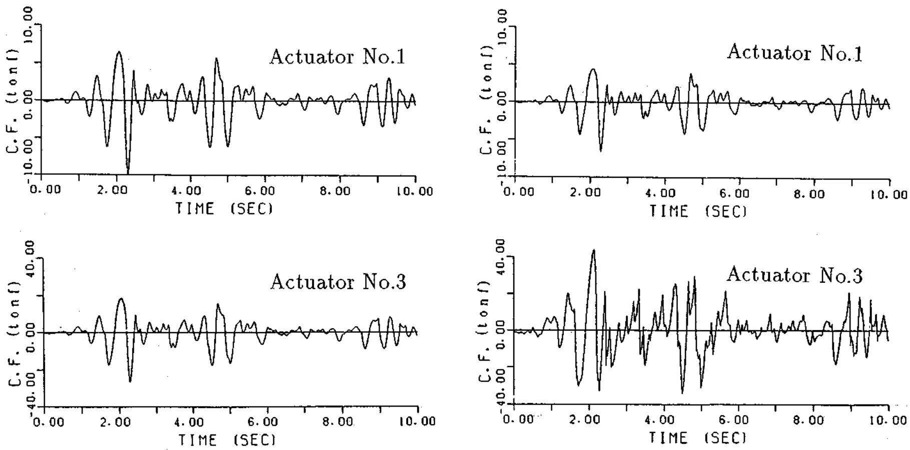

(a) results from Yang's control (b) results form our control

Fig. 3 Control forces from the top and bottom actuators.

$$\text{i) case 1}\quad \boldsymbol{Q}_{22}=\begin{bmatrix} 1.0 & 0.75 & 0.4 \\ 0.75 & 0.7 & 0.4 \\ 0.4 & 0.4 & 0.35 \end{bmatrix},\quad \text{ii) case 2}\quad \boldsymbol{Q}_{22}=\begin{bmatrix} 1.0 & 0.0 & 0.0 \\ 0.0 & 0.5 & 0.0 \\ 0.0 & 0,0 & 0.5 \end{bmatrix} \quad\cdots\cdots\cdots\cdots (17)$$

The maximum relative displacement of the top floor and the control force of the top actuator are expressed in **Fig. 4** as functions of $\beta Q_{11}/R_{11}$, in which β is a constant and Q_{11} and R_{11} the (1, 1) component of matrices $\boldsymbol{Q}_{11}$ and $\boldsymbol{R}$. Because Q_{11} and R_{11} are 1, the value of β can be used to represent $\beta Q_{11}/R_{11}$. Note that as β increases the structural response decreases consistently ; whereas, the required active control force increases. At the β of infinity the response becomes zero and the control force approaches a fixed value. The effect of the difference in the $\boldsymbol{Q}$ matrix appears in the control force. In some range of β the control force becomes larger than the asymptotic control force at infinite β when we select an inappropriate $\boldsymbol{Q}$ matrix.

The relation between α/R_{11} and the maximum relative displacement at the top floor, as well as the control force of the top actuator, is shown in **Fig. 5**. The maximum relative displacement and control force have minimum values at about $\alpha/R_{11}=10^2$ for a large range of β values. The decrease of the response is very sharp for small β values ; hence, the proposed control algorithm has a high efficiency for cases in which low capacity actuators are implemented.

Table 2 Comparison of control efficiencies.

		No Control	Yang's Control	Proposed Control
Max. Disp.(cm)	No1	5.629	2.797	1.948
	No2	3.679	1.947	1.163
	No3	2.012	1.075	0.6776
Max.	No1	-	9.918	6.606
Control (tonf)	No2	-	19.39	12.17
Force	No3	-	26.46	43.91
Input Energy (tonf*cm)		546.8	400.2	229.3
Control Energy (tonf*cm)		-	320.6	164.7

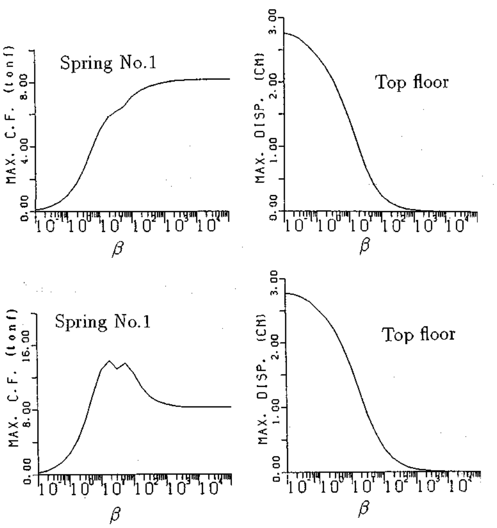

Fig. 4 Relation of β to the maximum relative displacement as well as to the control force (upper : with the $\boldsymbol{Q}_{22}$ matrix of case 1, lower : with the $\boldsymbol{Q}_{22}$ matrix of case 2).

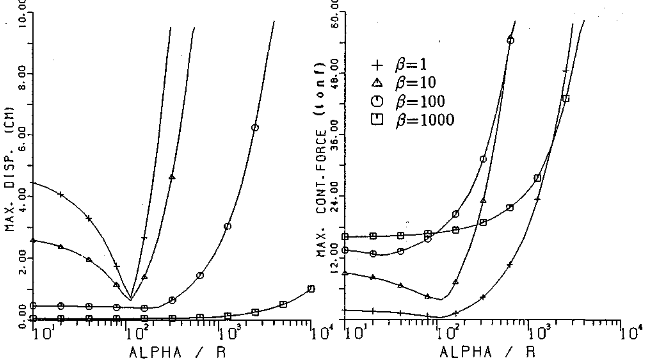

Fig. 5 Relation of α/R_{11} to the maximum relative displacement of the top floor and the maximum control force of the top actuator.

4. OPTIMAL CONTROL OF A NONLINEAR STRUCTURE

To treat the nonlinear problem of a structural system, the equation of motion is

$$\boldsymbol{M}\ddot{\boldsymbol{x}}(t)+\boldsymbol{C}\dot{\boldsymbol{x}}(t)+\boldsymbol{Y}(\boldsymbol{x}(t))=-\boldsymbol{m}\ddot{X}_0(t)+\boldsymbol{H}\boldsymbol{u}(t) \quad\cdots\cdots (18)$$

The difference between Eq. (1) and Eq. (18) is the restoring force term, the third term on the left side in both equations. To obtain the state space expression of Eq. (18), we decompose $\boldsymbol{Y}$ into the linear term $\boldsymbol{Kx}$ and the quasi-residual force $\boldsymbol{f}(t)$ at time t as follows:

$$\boldsymbol{Y}(\boldsymbol{x}(t))=\boldsymbol{K}(t)\boldsymbol{x}(t)+\boldsymbol{f}(t) \quad\cdots\cdots (19)$$

Substituting Eq. (19) into Eq. (18) the state space expression becomes

$$\dot{\boldsymbol{z}}(t)=\boldsymbol{A}\boldsymbol{z}(t)+\boldsymbol{F}_0(t)+\boldsymbol{B}\boldsymbol{u}(t)+\boldsymbol{W}_1\ddot{X}_0(t) \quad\cdots\cdots (20)$$

in which

$$\boldsymbol{F}_0(t)=\{0 \quad -\boldsymbol{M}^{-1}\boldsymbol{f}(t)\} \quad\cdots\cdots (21)$$

The solution of Eq. (20) is derived by a similar procedure to obtain Eq. (5) as

$$\boldsymbol{z}(t)=\boldsymbol{D}(t-\Delta t)+\frac{\Delta t}{2}[\boldsymbol{B}\boldsymbol{u}(t)+\boldsymbol{W}_1\ddot{X}_0(t)+\boldsymbol{F}_0(t)] \quad\cdots\cdots (22)$$

in which

$$\boldsymbol{D}(t-\Delta t)=e^{A}\Delta t\left\{\boldsymbol{Z}(t-\Delta t)+\frac{1}{2}[\boldsymbol{B}\boldsymbol{u}(t-\Delta t)+\boldsymbol{W}_1\ddot{X}_0(t-\Delta t)+\boldsymbol{F}_0(t-\Delta t)]\right\} \quad\cdots\cdots (23)$$

Minimizing the time-dependent performance index given in Eq. (9) under the constraint in Eq. (22) the optimal control solution $u(t)$ is

$$\boldsymbol{u}(t)=-\frac{\Delta t}{2}\boldsymbol{R}^{-1}\boldsymbol{B}'\boldsymbol{Q}\boldsymbol{z}(t)-\alpha\frac{\Delta t}{4}\boldsymbol{R}^{-1}\boldsymbol{B}'\boldsymbol{W}_2\ddot{X}_0(t) \quad\cdots\cdots (24)$$

The optimal control $\boldsymbol{u}(t)$ is not directly related to the system nonlinearity, being determined only from the system response and input acceleration at time t. The system nonlinearity is reflected in the control force through the feedback of the system response as expressed in the first term on the right side of Eq. (24). The coefficients of the state vector, z, and input motion, $\ddot{X}_0$, do not change with time. As they are defined by the control parameters and the mass distribution of the system, it does not take much computer time to calculate the control forces.

For illustrative purposes a three-story building similar to that shown in Fig. 1, but with the degrading trilinear characteristics of stiffness shown in Fig. 6 and Table 3, was modeled. For active tendon control $\beta=10$ with the matrix $\boldsymbol{Q}_{22}$ defined in case i) of Eq. (17) and $\alpha/R_{11}=40$ are used. The relative displacement of the top floor and the hysteresis loop of the inelastic restoring force of the top spring are shown in Fig. 7; lower shows results without active control and upper with control. The control forces for the top and bottom actuators are presented in Fig. 8. Both figures show that the maximum displacement is reduced more than 50 %; but the maximum restoring force by only 20 %. A comparison of Fig. 8 with Fig. 3

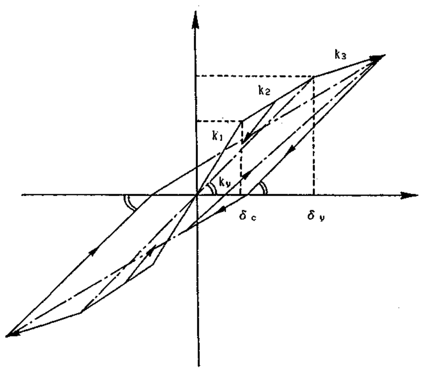

Fig. 6 Degrading trilinear characteristics.

Table 3 Structural properties of a nonlinear model.

NO.	Mass (ton)	Stiffness (tonf/cm) K0	K1	K2	Crack point (cm)	Yield point (cm)
1	0.048	23.60	K0/3	K0/10	0.25	0.5
2	0.048	42.59	K0/3	K0/10	0.25	0.5
3	0.048	47.32	K0/3	K0/10	0.25	0.5

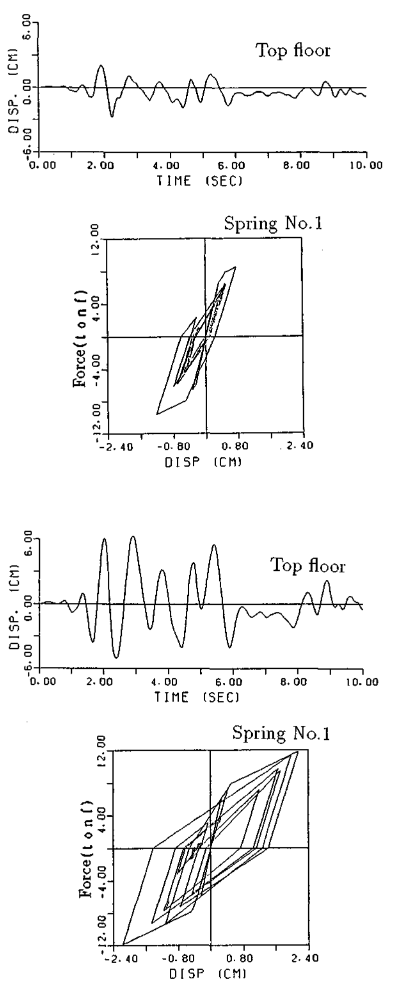

Fig. 7 Relative displacement of the top floor and the restoring force of the top spring (upper : with, lower : without control).

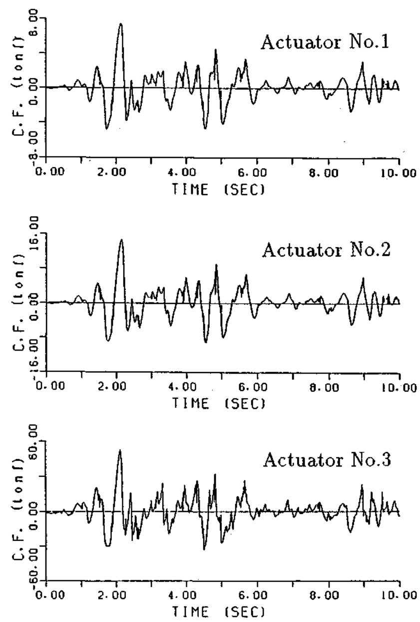

Fig. 8 Control forces of the actuators.

shows that the control force of the top actuator does not differ much ; whereas, the force of the bottom actuator for the nonlinear system is 45 % larger than that for the linear one. Based on our algorithm the control is defined only from the system response and the input acceleration ; therefore, a large control force is needed for the nonlinear system because the system response usually is larger than for a linear one. Moreover, numerical results indicate that the response of the entire system can be brought back to the elastic range by increasing the control force.

5. OPTIMAL CONTROL OF A BASE-ISOLATED STRUCTURE

A three-story building resting on laminated rubber bearings with a lead core is modeled. Bacause the effect of the rubber isolator introduces a soft story with inelastic characteristics, the superstructure behaves like a rigid body and the relative displacement between stories become very small ; whereas, the relative displacement between the superstructure and the ground becomes very large. Active tendon control is introduced to limit the relative displacement of the rubber isolator to avoid instability failure as well as the relative displacement of the superstructure. The dynamic characteristics of the superstructure are assumed to be linear elastic (Table 1) ; whereas, the rubber isolator has bilinear elastic-plastic behavior. The elastic stiffness of the base isolator is assigned as 2.2 tf/cm and the post-elastic stiffness 0.44 tf/cm. Yielding is assumed to occur at a relative displacement of 0.5 cm. As the total system has been modeled as a four-degree-of-freedom system we use matrix $\boldsymbol{Q}_{22}$ as defined by

$$\boldsymbol{Q}_{22}=\begin{bmatrix} 1.0 & 0.7 & 0.4 & 0.2 \\ 0.7 & 0.7 & 0.4 & 0.2 \\ 0.4 & 0.4 & 0.4 & 0.2 \\ 0.2 & 0.2 & 0.2 & 0.2 \end{bmatrix} \qquad (25)$$

The values of β and α/R_{11} are assigned as 100 and 40.

The controlled and uncontrolled relative displacements of the top floor and base isolator with respect to the ground are shown in Fig. 9. The hysteresis loops of the elastic-plastic restoring shear forces in the base isolator are shown in Fig. 10; (a) represents a case without control and (b) with it. These figures show that the active tendon control system markedly reduces not only the superstructure response but the deformation of the base isolator as well. As a check on increases in the relative displacement between stories, the force-relative displacement relation of the top spring is given in Fig. 11. Even if the control force is applied to the structural system, the relative displacement between the top and second floors is kept very small. The base isolation system is used to absorb a large deformation and to dissipate input energies such that smaller excitations are transmitted to the superstructure. This system, however, must be protected against severe damage or instability failure. This is achieved by the ability of our proposed optimal control algorithm to reduce deformation of the base isolator and to maintain a small relative displacement between the stories.

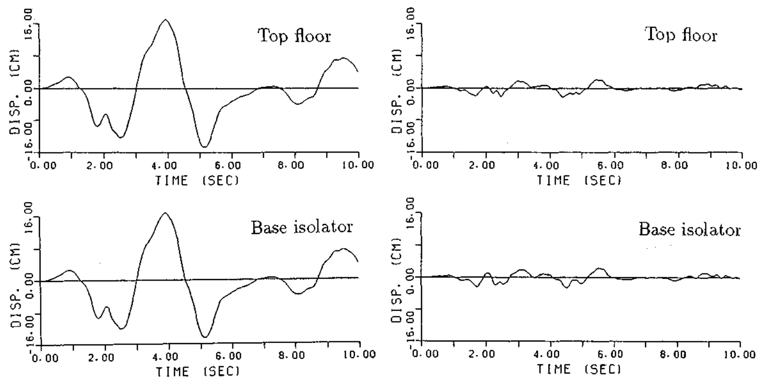

(a) without control (b) with control

Fig. 9 Relative displacement to the ground.

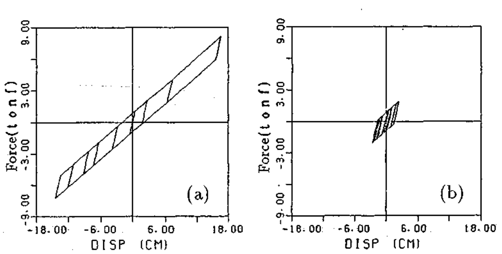

(a) without (b) with control

Fig. 10 Hysteresis loops of the base isolator.

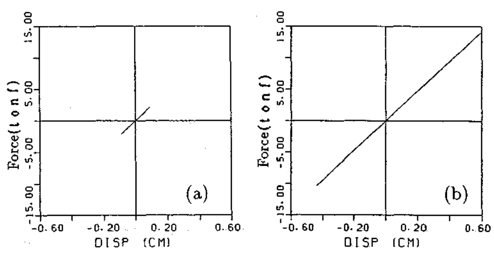

(a) without (b) with control

Fig. 11 Force-displacement relation of the top spring.

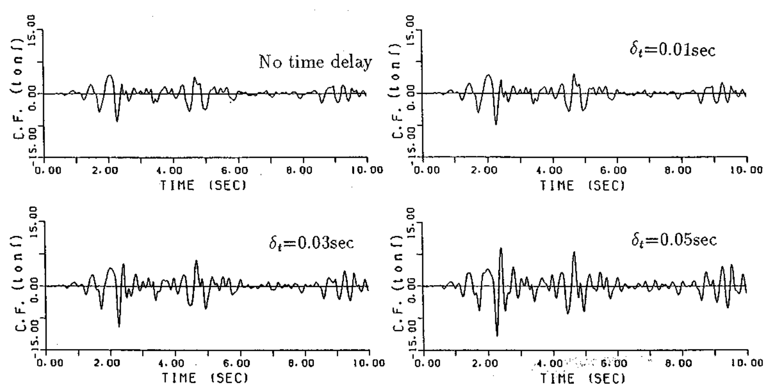

Fig. 12 Relative displacement for various time delays of control.

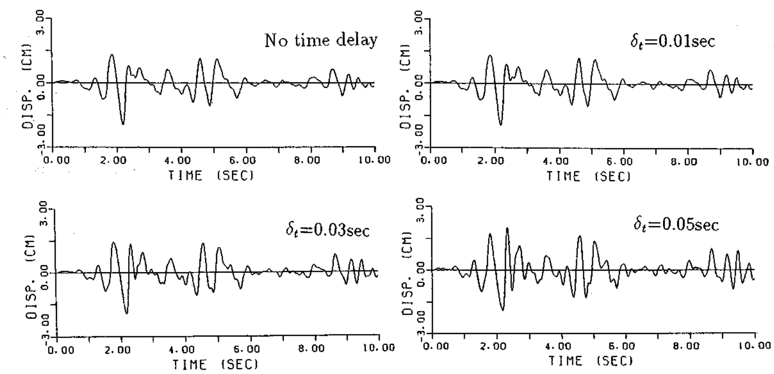

Fig. 13 Control force for various time delays of control.

6. TIME DELAY OF THE CONTROLLING FORCE

To apply the developed continuous-time control algorithms to a real structural system we must take into account the time delay not only for digitizing the observed input motion and system response but for calculating the control force and for applying it in the form of stepwise functions through A/D converters.

We assume that the optimal control algorithm is not affected even if the control force is applied to the system with a time delay of δt ; hence, the control vector $u(t)$ has the same form as given in Eqs. (14) or (24). The only difference is in the state vector $z(t)$ in which $u(t)$ is replaced by $u(t-\delta t)$. The same structure model and control parameters that are assumed in nonlinear analyses are used. The unit time delay for controlling the system is assumed to be 0.01 sec. The relative displacement of the top floor and the control force of the top actuator are shown for one, three, and five unit time delays in Figs. 12 and 13. The system response and control force become large as the time delay increases ; but, the system response does not have a large effect for 0.01 sec delay of the controlling force. If the response time of the tendon actuator is within several units of time delay, the efficiency of the proposed algorithm is confirmed. With this in mind, discrete-time formulations of active structural control must be developed which include the discussion of time delay compensation.

7. CONCLUSIONS

We have developed a new closed-open-loop active control algorithm which takes into account the input seismic energy to the structure system. We investigated the efficiency of our proposed control algorithm by applying it to linear and nonlinear structural systems with, and without , a base isolator. The time delay of the controlling force also was studied. The principle results and conclusions of our study are

(1) The effect of control parameters on the system response are expressed by two independent variables ; one controls the level of feedback, the other reflects the level of input excitation. For a given structural system we found that there were appropriate control parameters to maximize control efficiencies.

(2) The combination of passive and active control systems is of use in preventing the failure of the base isolator while simultaneously keeping the relative displacement of the superstructure parts small. Because a base isolator absorbs seismic input and behaves nonlinearly, the optimal algorithm we have developed, which includes the effect of seismic excitation, is very efficient for the control of a building with a base isolation system.

(3) The effect of time delay to apply the control force to the system has been investigated. As the time delay increases, the system response and control force become large and unstable.

REFERENCES

1) Soong, T. T. : Active Structural Control in Civil Engineering, National Center for Earthquake Engineering Research, Technical Report NCEER-87-0023, State University of New York at Buffalo, 1987.
2) Leipholz, J. N. : Structural Control, North-Holland Publishing Company, Amsterdam, The Netherlands, 1980.
3) Bryson, A. E. Hr and Ho, Y. C. : Applied Optimal Control, John Wiley and Sons, New York, U. S. A., 1975.
4) Yang, J. N., Akbarpour, A. and Ghaemmaghami, P. : New Optimal Control Algorithms for Structural Control, Journal of Engineering Mechanics, ASCE, Vol. 113, No. 9, pp. 1369-1386, 1987.
5) Udwadia, F. E. and Tabaie, S. : Pulse Control of Structural and Mechanical Systems, Journal of Engineering Mechanics, ASCE, Vol. 107, No. 6, pp. 1011-1028, 1981.

(Received July 15 1989)